RSC Advances

PAPER

View Article Online
View Journal | View Issue

Cite this: *RSC Adv.*, 2025, **15**, 6974

Catalytic reduction of nitrophenols and dyes by HKUST-1/hydrogel composite

Atipong Nachaichot,[a] Orrawin Kenvised,[a] Sirikanlaya Choram,[a] Supinya Nijpanich[b] and Surangkhana Budsombat*[a]

The effective removal of nitrophenols from wastewater is crucial due to their high carcinogenic risk. This research presents the development of a copper-based metal–organic framework (HKUST-1) integrated into a chitosan-*graft*-poly(acrylic acid) hydrogel. The hydrogel composite was evaluated as a catalyst for reducing nitrophenols and dyes using sodium borohydride ($NaBH_4$) as a reducing agent. Various conditions were investigated for the reduction of 4-nitrophenol (4-NP) to the less harmful 4-aminophenol (4-AP), including catalyst dosage, $NaBH_4$ concentration, initial 4-NP concentration, temperature, and pH. The catalyst was able to completely reduce 4-NP within 25 minutes at a dosage of 3 g L^{-1} and a $NaBH_4$ concentration of 300 mM. The reduction rate increased with higher temperatures, with an Arrhenius activation energy of 54.4 kJ mol^{-1}. Common anions found in surface water, such as Cl^-, NO_3^-, SO_4^{2-}, and HCO_3^-, had a slight impact on the reduction rate of 4-NP. When tested in real water environments, the reduction rate decreased, but complete conversion was still achieved. Additionally, the composite successfully reduced 100% of 2-nitrophenol, 100% of methyl orange, and 69% of Congo red. Overall, the hydrogel composite has shown significant potential as a catalyst for reducing various organic pollutants with high efficiency and easy separation through filtration.

Received 5th January 2025
Accepted 25th February 2025

DOI: 10.1039/d5ra00081e

rsc.li/rsc-advances

1. Introduction

Due to the expansion of urbanization and industrialization, hazardous substances have been released into water environments. Nitrophenols, which are used in pesticides, explosives, pharmaceuticals, and dyes,[1] are categorized as toxic pollutants by the United States Environmental Protection Agency (US EPA).[2] The discharge of nitrophenols can be harmful to human health due to their high carcinogenic potential.[3] As a result, developing effective methods for removing nitrophenols has become a significant area of interest. Additionally, the reduction of nitrophenols yields valuable aminophenols, which are useful in the pharmaceutical industry.

Several approaches, including photodegradation and Fenton oxidation, have been employed to remove nitrophenols.[4] Recently, 4-nitrophenol (4-NP) has been successfully reduced to 4-aminophenol (4-AP) using metal catalysts such as silver, gold, nickel, platinum, cobalt, and copper in combination with sodium borohydride ($NaBH_4$) as a reducing agent.[5–8] These metal catalysts facilitate the electron transfer from borohydride (BH_4^-) as an electron donor to nitrophenol as an electron acceptor.[9] Copper (Cu) is considered a promising catalyst for the reduction of 4-NP due to its low cost, lower toxicity, and effectiveness.[10,11] However, the use of homogeneous catalysts is limited because of the leaching of metal ions.

HKUST-1 is a copper-based metal–organic framework (MOF) composed of benzene-1,3,5-tricarboxylic acid (BTC) and dimeric cupric tetracarboxylate units. It was first synthesized at the Hong Kong University of Science and Technology.[12] HKUST-1 has been utilized as a catalyst in chemical processes such as esterification, hydrogenation, and reduction. Additionally, it has proven to be an effective adsorbent for 4-NP with high water stability.[13] In previous studies, HKUST-1 was embedded in functionalized SBA-15 [14] and mesoporous silica nanospheres,[15] resulting in composite materials that exhibited high catalytic activity for the reduction of 4-NP.

In this work, chitosan-*graft*-poly(acrylic acid) (CS-*graft*-PAA) hydrogel was synthesized and used as an adsorbent for Cu^{2+} ions due to its high adsorption capacity attributed to its multifunctional groups.[16] To stabilize the Cu^{2+} ions adsorbed in the hydrogel, the Cu^{2+} ions were converted into HKUST-1. The HKUST-1/hydrogel composite was then used as a catalyst for reducing 4-NP. The three-dimensional network of the hydrogel was designed to provide excellent dispersion of the catalyst, thereby enhancing its catalytic performance. Moreover, the heterogeneous catalyst can be easily recovered through filtration. Various reduction parameters were investigated, including catalyst dosage, $NaBH_4$ concentration, initial concentration of 4-NP, temperature, and solution pH. The performance of the catalyst

[a]*Department of Chemistry and Center of Excellence for Innovation in Chemistry, Faculty of Science, Khon Kaen University, Khon Kaen 40002, Thailand. E-mail: surama@kku.ac.th; Fax: +66 432 02373; Tel: +66 432 02222-12243*

[b]*Synchrotron Light Research Institute (Public Organization), Nakhonratchasima 30000, Thailand*

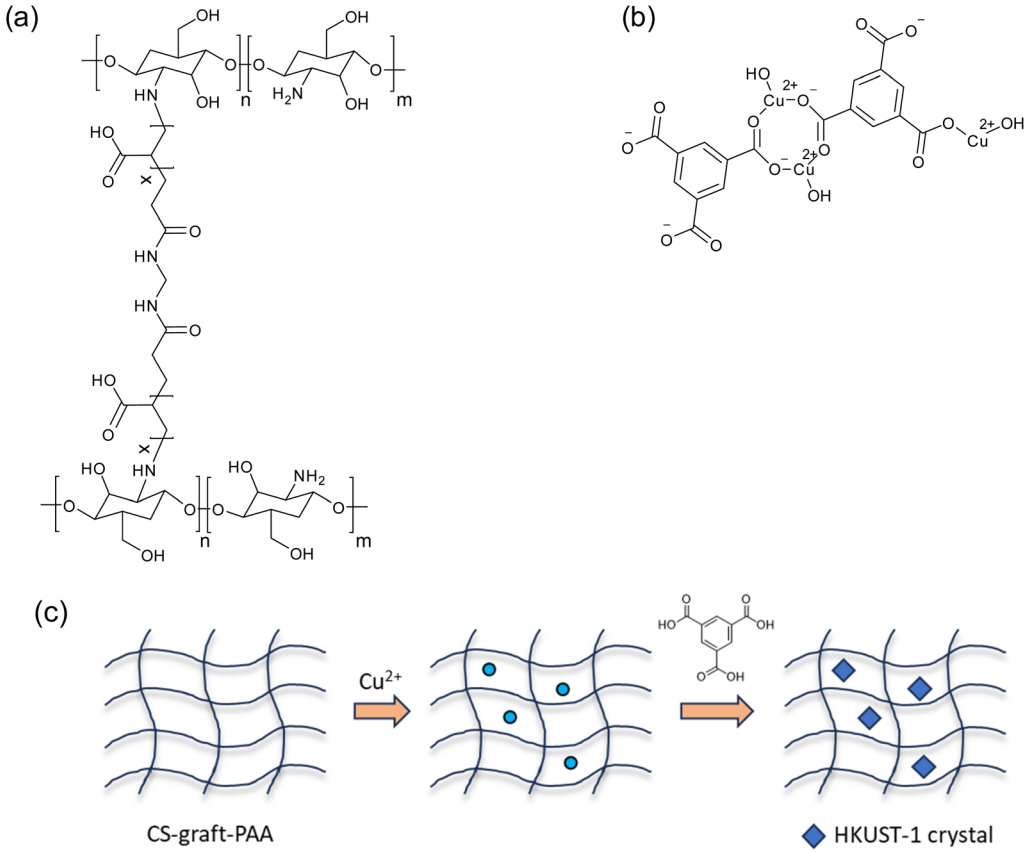

Scheme 1 Chemical structures of CS-*graft*-PAA hydrogel (a) and HKUST-1 (b). (c) Schematic representation of the *in situ* synthesis of HHKUST-1 in the hydrogel.

was evaluated in the presence of common anions and in real water environments. Additionally, the catalyst was tested for the reduction reaction of 2-nitrophenol (2-NP) and two dye models—methyl orange and Congo red. This study represents the first example of the *in situ* synthesis of HKUST-1 within a Cu^{2+}-containing hydrogel and demonstrates the circular reutilization of secondary waste for catalytic reduction.

2. Experimental

2.1 Chemicals

4-NP (98%) was sourced from Acros Organics (Belgium). 2-NP (99%), chitosan (50 000–190 000 Da), and acrylic acid (AA, 99%) were purchased from Sigma-Aldrich (USA). BTC (98%) was obtained from TCI (Japan). Copper(II) nitrate trihydrate ($Cu(NO_3)_2 \cdot 3H_2O$, 99.5%), $NaBH_4$ (95%), and Congo red were supplied by Loba Chemie (India). Methyl orange was acquired from Carlo Erba Reagents (Thailand). Potassium persulfate (99%) was purchased from VWR (Thailand). *N*,*N*′-Methylenebis(acrylamide) (MBA, 98%) was acquired from Fluka (USA).

2.2 Preparation of HKUST-1 composite

The CS-*graft*-PAA hydrogel was synthesized following previously reported procedures.[16] Initially, partial neutralization of 10.00 g of AA was conducted using a sodium hydroxide solution. Then, 0.45 g of chitosan, 0.02 g of MBA, and 0.04 g of potassium persulfate were added to the solution. The mixture was stirred and purged with nitrogen. Polymerization took place at 50 °C for 2.5 hours. Afterward, the hydrogel was cut into small pieces, thoroughly washed with water to remove residual chemicals, and then dried in an oven.

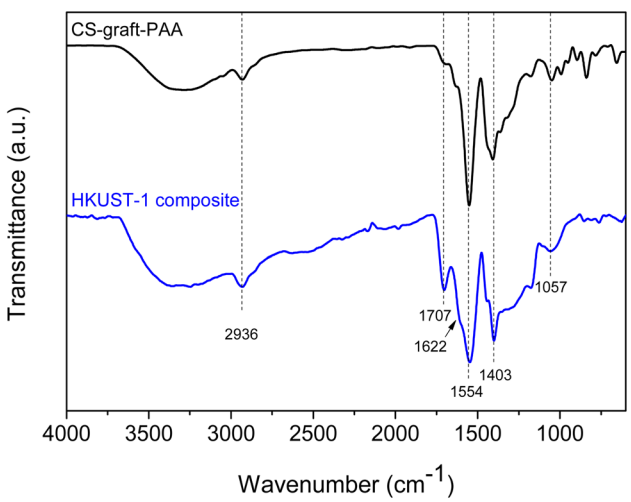

Fig. 1 ATR-FTIR spectra of CS-*graft*-PAA and HKUST-1 composite.

HKUST-1 was synthesized *in situ* within the hydrogel as follows: first, 3.77 g of $Cu(NO_3)_2 \cdot 3H_2O$ was dissolved in 151 mL of deionized water. The hydrogel (9.97 g) was immersed in the Cu^{2+} solution for 5 hours. The hydrogel was taken out and immersed in a 200 mL solution of BTC for 12 hours. The molar ratio of BTC to $Cu(NO_3)_2 \cdot 3H_2O$ was 1.2. Finally, the hydrogel was removed from the BTC solution and washed with water. The resulting composite was then dried in an oven.

2.3 Catalytic reduction experiment

A typical catalytic reduction experiment for 4-NP was conducted as follows: a composite catalyst (1–3 g L^{-1}) was added to a solution of 4-NP (10–20 mM). The mixture was stirred for 30 minutes to reach adsorption–desorption equilibrium. The reduction reaction was initiated by adding a 300 mM $NaBH_4$ solution. At specific time intervals, samples were withdrawn from the solution, diluted with deionized water, and then

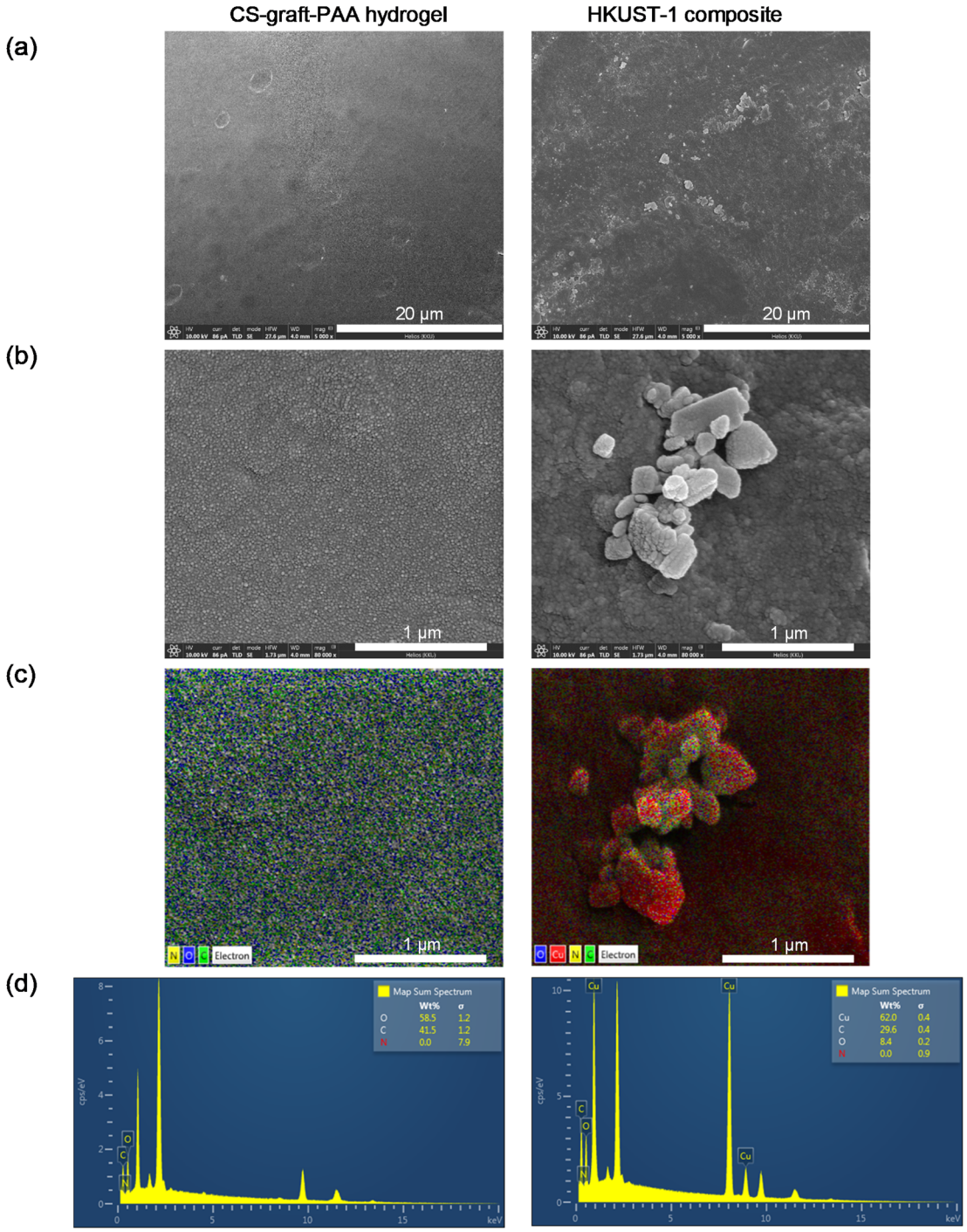

Fig. 2 FESEM images at (a) 5000× and (b) 80 000× magnifications. (c) Elemental mappings and (d) compositions of CS-*graft*-PAA hydrogel and HKUST-1 composite (80 000×).

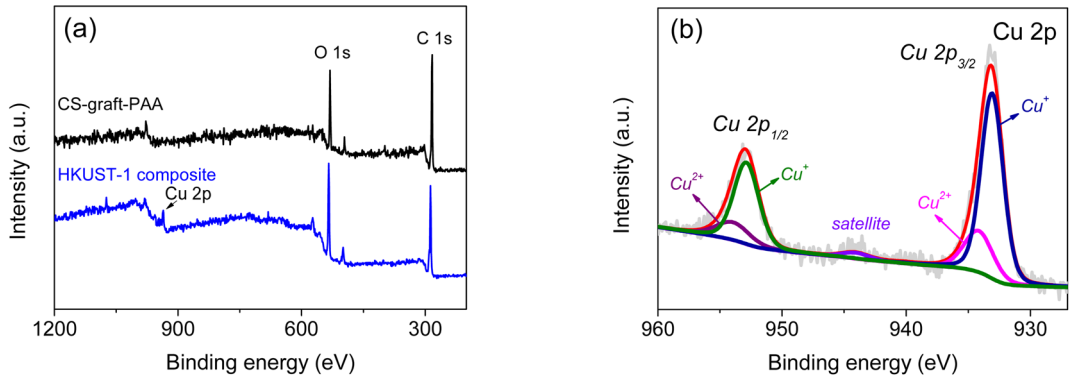

Fig. 3 (a) Survey XPS spectra of CS-*graft*-PAA hydrogel and HKUST-1 composite and (b) Cu 2p spectra of HKUST-1 composite.

analyzed using ultraviolet-visible (UV-vis) spectroscopy. The conversion of 4-NP to 4-AP was calculated using the absorbances at times 0 (A_0) and t (A_t) using eqn (1).

$$\text{Conversion}(\%) = \frac{A_0 - A_t}{A_0} \times 100 \quad (1)$$

Additionally, the catalytic performance of the catalyst was evaluated in the presence of 5 mM common anions and in actual water environments. The pond water used in the experiments was collected from a wastewater treatment pond at Khon Kaen University. The reduction of other organic pollutants was monitored at their respective maximum wavelengths.

2.4 Characterizations

The surface morphology of the HKUST-1 composite was examined using a field emission scanning electron microscope equipped with an energy-dispersive X-ray spectroscope (FESEM-EDS, Helios NanoLab G3 CX, FEI, Australia). The functional groups present in the CS-*graft*-PAA and HKUST-1 composite were analyzed using a Bruker attenuated total reflection Fourier transform infrared spectrometer (ATR-FTIR, Tensor 27, Germany). Thermal analysis was performed under a nitrogen atmosphere using a thermogravimetric analyzer (TGA, STA7200, Hitachi, Japan) with a heating rate of 10 °C per minute. An X-ray diffractometer (XRD, EMPYREAN, PANalytical, United Kingdom) was used to examine the crystallinity of the samples. A UV-vis spectrophotometer (Agilent 8453, USA) was used to analyze the concentration of 4-NP and other pollutants. Liquid chromatography-mass spectrometry (LC-MS, Waters, Xevo TQ-XS, USA) was performed for mass analysis. The method utilized a gradient of methanol and a 2.5 mM ammonium acetate solution, with a flow rate of 0.3 mL per minute. The electronic properties of the HKUST-1 composite were studied using an X-ray photoelectron spectroscope (XPS, PHI5000 VersaProbe II, ULVAC-PHI, Japan).

3. Results and discussions

3.1 Preparation of HKUST-1 composite

The CS-*graft*-PAA hydrogel was first synthesized *via* free radical grafting of AA onto chitosan, using MBA as a crosslinking agent. Subsequently, an *in situ* synthesis of HKUST-1 was conducted within the hydrogel. The chemical structures of the CS-*graft*-PAA hydrogel and HKUST-1 are shown in Scheme 1(a) and (b), respectively. Moreover, the schematic representation of the *in situ* synthesis of HHKUST-1 in the hydrogel is provided in Scheme 1(c). As a result, the yellow color of the hydrogel changed to blue. Both the pristine hydrogel and the HKUST-1

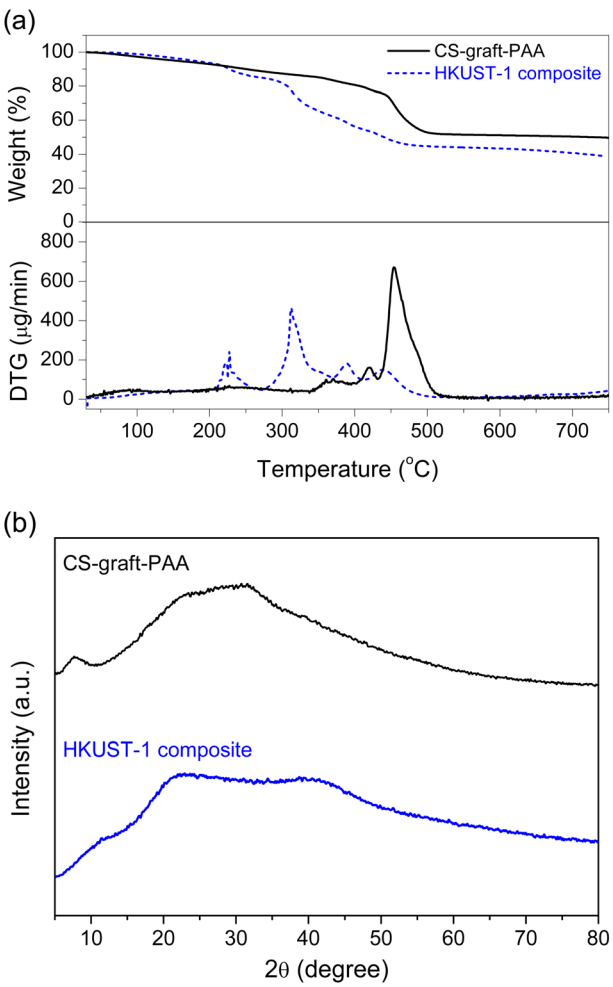

Fig. 4 (a) TGA thermograms and (b) XRD patterns of CS-*graft*-PAA and HKUST-1 composite.

composite were characterized using ATR-FTIR, FESEM with EDX, XPS, and TGA.

Fig. 1 illustrates the FTIR spectra of the pristine hydrogel and the composite. The pristine hydrogel displays characteristic bands for N–H bending and in-plane CH_2 bending or scissoring of MBA at 1554 cm^{-1} and 1403 cm^{-1}, respectively.[17] Additionally, the O–H bending of a primary alcoholic group in chitosan is evident at 1057 cm^{-1}, along with the $-CH_2$ stretching observed at 2936 cm^{-1}.[18] For the composite, bands corresponding to the aromatic C=C and COO^- of BTC in HKUST-1 are located at 1622 cm^{-1} and 1707 cm^{-1}, respectively.[13]

Fig. 2(a)–(d) present FESEM images with elemental mappings and compositions of the pristine hydrogel and the HKUST-1 composite. The non-uniform size and irregular shape of HKUST-1 possibly result from competitive covalent bonding between $Cu(NO_3)_2$ and CS-*graft*-PAA and BTC.[19] The elemental mapping indicates that carbon, oxygen, and Cu are dispersed throughout the composite surface, with the weight percentage of Cu determined to be 62.0%.

The survey XPS spectra of the pristine hydrogel and the HKUST-1 composite are presented in Fig. 3(a). For the pristine hydrogel, the C 1s peak and the O 1s peak, originating from chitosan and PAA, appear at 284.3 eV and 532.4 eV, respectively.[16] The Cu 2p spectrum confirms the presence of HKUST-1 in the composite. As illustrated in Fig. 3(b), the 953.0 eV and 933.2 eV peaks corresponded to the Cu $2p_{1/2}$ and Cu $2p_{3/2}$ levels, respectively. Each peak has been deconvoluted into two forms of copper ions: monovalent (Cu^+) and divalent (Cu^{2+}).[20] These results indicate the existence of both Cu^{2+}/Cu^{2+} paddle-wheel arrangements and Cu^+/Cu^{2+} paddle-wheel defects.[21] Additionally, a small Cu^{2+} shake-up satellite peak is observed at 944.1 eV.[22]

TGA thermograms of the pristine hydrogel and the composite are shown in Fig. 4(a). Below 120 °C, both samples exhibit slight weight loss due to the loss of absorbed water. The pristine hydrogel displays a complex thermogravimetric profile, with a primary weight loss occurring around 450 °C, attributed to the decomposition of poly(acrylic acid) within the hydrogel.[16] The HKUST-1 composite shows thermal stability up to approximately 200 °C, followed by a sharp weight loss at 300 °C, which is attributed to the transformation of $Cu_3(BTC)_2$ to CuO.[23] The content of HKUST-1 in the hydrogel was calculated based on the difference in residual weights, yielding a value of 11.2%.

XRD was used to examine the crystallinity of the pristine hydrogel and the HKUST-1 composite. As shown in Fig. 4(b), the XRD pattern of the pristine hydrogel was broad between 15–45°, which was due to a random crosslinking network.[24] No sharp characteristic peaks of HKUST-1 at 16.1°, 16.9°, 18.8°, 19.5°, 21.3°, 22.8°, 25.2°, 26.1°, 30.3°, and 33.8° were observed for the composite.[25] This could be attributed to the relatively low HKUST-1 content and the peak overlap with those of the pristine hydrogel.

3.2 Reduction of 4-NP

3.2.1 Effect of catalyst dosage. The HKUST-1 composite was evaluated as a catalyst for reducing 4-NP in the presence of an excess of the reducing agent, $NaBH_4$. Fig. 5(a) shows the UV-vis absorption spectra of 4-NP solutions with $NaBH_4$ and the composite catalyst over time. In the mechanism of the catalytic reduction reaction, $NaBH_4$ undergoes hydrolysis, leading to an increase in the solution pH. In an alkaline medium, 4-NP is converted into its corresponding 4-nitrophenolate ion.[26] As the reaction progressed, the intensity of the peak at 400 nm, corresponding to 4-nitrophenolate, decreased, and a peak at 300 nm, associated with 4-AP, gradually increased. The presence of isosbestic points at 280 nm and 316 nm indicates that no side reactions occurred during the reduction of 4-NP to 4-AP.[27] An LC-MS analysis was performed to confirm the reduction of 4-NP to 4-AP. Fig. 5(b) presents the MS spectra of the solution containing 4-NP and $NaBH_4$ in the presence of the composite catalyst at two different time intervals: at the beginning of the reaction (after 15 seconds) and after 40

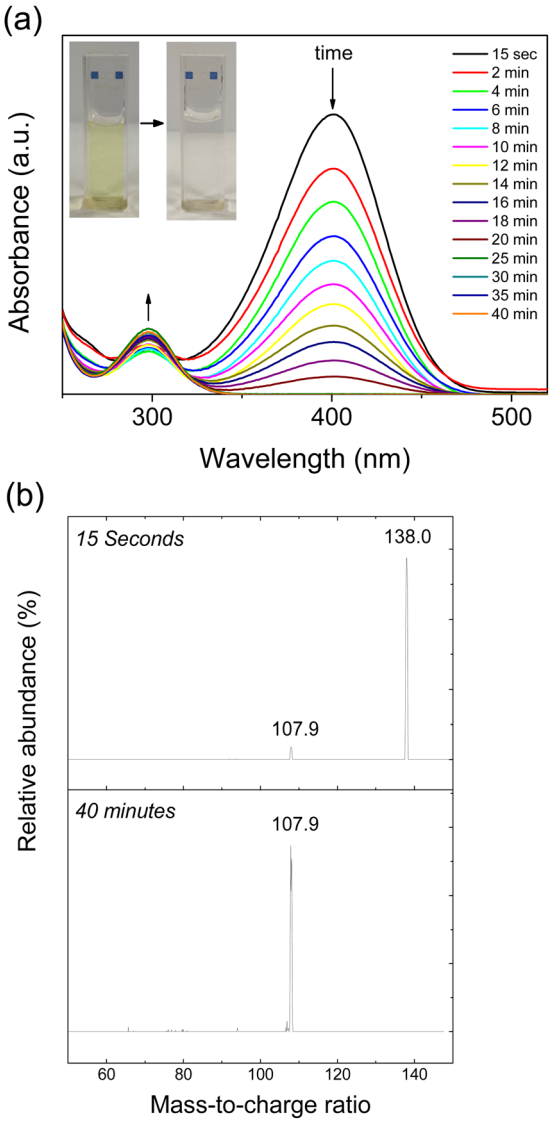

Fig. 5 (a) UV-visible absorption spectra of the reduction of 4-NP to 4-AP using HKUST-1 composite over time. The inset shows the change of color after reduction. (b) MS spectra of the solution of 4-NP and $NaBH_4$ at different time intervals.

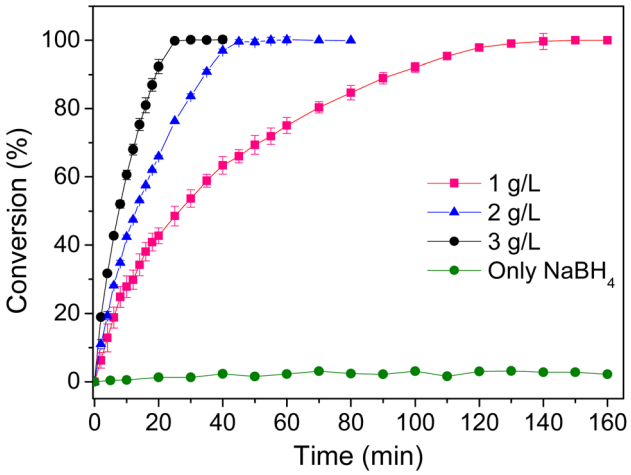

Fig. 6 Effect of catalyst dosage. Condition: [4-NP] = 15 mM; [$NaBH_4$] = 300 mM.

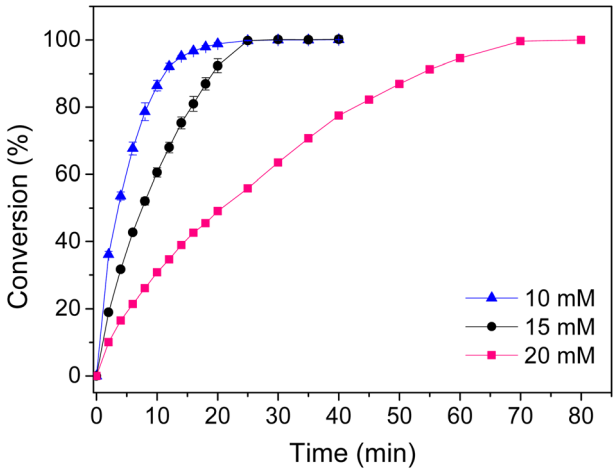

Fig. 8 Effect of initial 4-NP concentration. Condition: [cat.] = 3 g L^{-1}; [$NaBH_4$] = 300 mM.

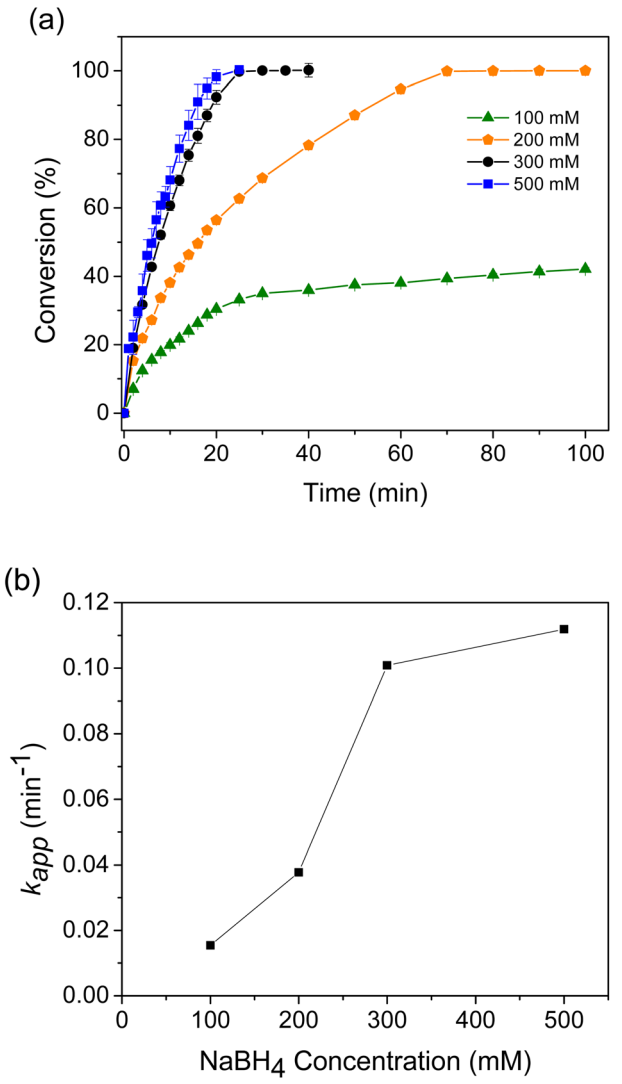

Fig. 7 (a) Effect of $NaBH_4$ concentration and (b) rate constants for 4-nitrophenol reduction. Condition: [cat.] = 3 g L^{-1}; [4-NP] = 15 mM.

minutes. Initially, a prominent peak with a mass-to-charge ratio (m/z) of 138.0, corresponding to the molecular weight of 4-NP,[28] was observed. Additionally, a small peak with an m/z of 107.9, corresponding to the molecular weight of 4-NP, appeared due to a rapid reduction that occurred during sample preparation before the injection into the instrument. After 40 minutes of reduction, only one peak corresponding to 4-AP was detected. The mechanism proposed for the reduction of 4-NP using the HKUST-1 composite can be described as follows: both 4-NP and BH_4^- are adsorbed onto the surface of the HKUST-1 composite through pi–pi stacking interactions. The BH_4^- ions then bind to the Cu active sites, forming Cu-based hydride complexes. These hydride complexes subsequently transfer electrons to 4-NP to form 4-AP, which is later desorbed from the catalyst.[15] Additionally, the influence of catalyst dosage on the reduction of 4-NP was studied. As shown in Fig. 6, only 3% of 4-NP was reduced when only $NaBH_4$ was used. The reduction rate was significantly enhanced in the presence of both $NaBH_4$ and the composite catalyst. The rate increased with higher catalyst dosages due to a greater number of available active sites.[29] At a catalyst dosage of 3 g L^{-1}, 4-NP was completely reduced after 25 minutes.

3.2.2 Effect of $NaBH_4$ concentration. The effect of $NaBH_4$ concentration on the reduction of 4-NP was investigated. As shown in Fig. 7(a), the reduction rate increased with higher concentrations of $NaBH_4$. The reduction of 4-NP is considered to be pseudo-first-order since there is an excess of $NaBH_4$ present. Consequently, the apparent rate constant (k_{app}) was determined using the following equation:[3]

$$\ln\frac{A_t}{A_0} = -k_{app}t \quad (2)$$

As illustrated in Fig. 7(b), the k_{app} value increased with rising $NaBH_4$ concentrations and eventually leveled off at 300 mM. This indicates that a $NaBH_4$ concentration of 300 mM is sufficient for the reduction of 4-NP and was therefore used in subsequent investigations.

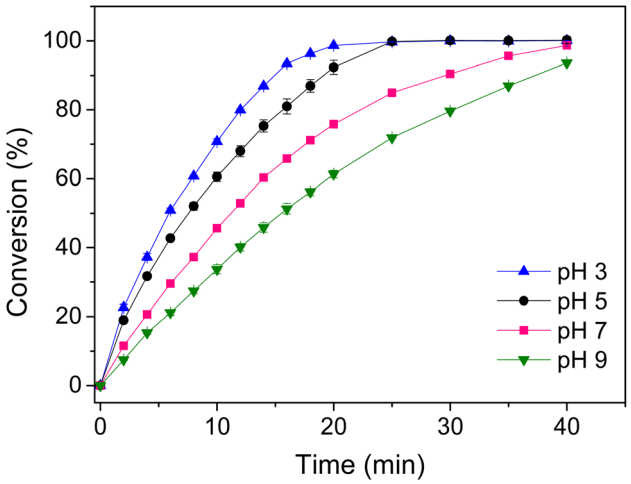

Fig. 9 Effect of solution pH. condition: [cat.] = 3 g L^{-1}; [4-NP] = 15 mM; [$NaBH_4$] = 300 mM.

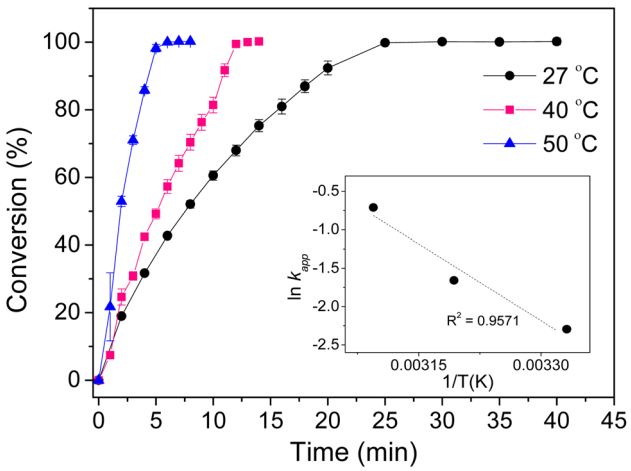

Fig. 10 Effect of temperature. Condition: [cat.] = 3 g L^{-1}; [4-NP] = 15 mM; [$NaBH_4$] = 300 mM.

3.2.3 Effect of 4-NP concentration. The catalytic efficiency of the HKUST-1 composite was examined at initial concentrations of 4-NP ranging from 10 to 20 mM. As shown in Fig. 8, at the lower concentration of 10 mM, the reduction occurred rapidly, completing within 20 minutes. However, as the initial concentration of 4-NP increased, the reduction rate declined. This decrease is attributed to the high competition among 4-NP molecules for the limited active sites available on the catalyst. Additionally, the adsorption of either 4-NP or its reduction product, 4-AP, on the catalyst's surface could hinder the approach of borohydride ions.[3] Despite the slower reduction rate at 20 mM, a 100% conversion was still achieved within 80 minutes.

3.2.4 Effect of pH. The influence of pH on the reduction of 4-NP was studied within a range from 3 to 9. Fig. 9 illustrates that the reduction rate decreased as the pH value increased. Additionally, the conversion slightly dropped from 100% to 94% when the pH was raised from 3 to 9. The catalyst displayed high efficiency at lower pH levels. The hydrolysis of $NaBH_4$ involved two steps: hydrolysis of water molecules (eqn (3)) and hydrolysis of borohydride ions (eqn (4)).[4,30]

$$H_2O \leftrightarrow H^+ + OH^- \quad (3)$$

$$H^+ + BH_4^- + 3H_2O \leftrightarrow H_3BO_3 + 2H_2 \quad (4)$$

The hydrolysis of borohydride ions occurs more slowly than the hydrolysis of water molecules, making it the rate-determining step in the reaction. At lower pH values, protons in solution readily bond with the hydrogen atoms in borohydride ions, resulting in a faster hydrolysis of the borohydride ions and an accelerated reduction of 4-NP.[31] Under alkaline conditions, the available protons for reactions were reduced; therefore, the hydrolysis rate decreased. A similar observation has been reported for the catalytic reduction of 4-NP using heterostructured gold-magnetite nanocatalysts.[4]

3.2.5 Effect of temperature. The effect of temperature on the reduction of 4-NP was investigated. Fig. 10 demonstrates that as the temperature increases, the reduction rate also increases due to a higher diffusion rate of the reactants.[10] To calculate the Arrhenius activation energy (E_a), a plot of $1/T$ against ln k_{app} was constructed. As shown in the inset of Fig. 10, E_a was calculated from the slope of this plot and found to be 54.4 kJ mol^{-1}. It has been noted that the activation energy for diffusion-controlled reactions is typically below 20 kJ mol^{-1}, while that for reaction-controlled processes is higher.[32] Therefore, the reduction of 4-NP using the HKUST-1 composite can be classified as a reaction-controlled process, where the rate-determining step involves the electron transfer between 4-NP

Table 1 Comparison with other monometallic MOFs-based catalysts for the reduction of 4-NP

Catalyst	Reaction condition [4-NP]; [catalyst]; [$NaBH_4$]	Performance conversion; time	References
Co-BDC	20 ppm; 5 mg; 0.13 mM	99.25%; 2 min	33
Carbonized Fe-BDC	20 ppm; 5 mg/4 mL; 0.5 M	100%; 4 min	34
NH_2-MIL-101(Fe)	20 ppm; 0.5 g L^{-1}; 0.5 M	100%; 4 min	35
HKUST-1@SBA-15C (1/8)	0.09 mM; 1 mg; 30 mM	100%; 7.5 min	14
HKUST-1@MSN-NH_2	~50 μM; 2.5 g L^{-1}; 30 mM	100%; 10 min	15
C-HK(Cu)	2 mM; 0.1 g L^{-1}; 40 mM	~65%; 40 min	36
HKUST-1/hydrogel	15 mM; 3 g L^{-1}; 300 mM	100%; 25 min	This work

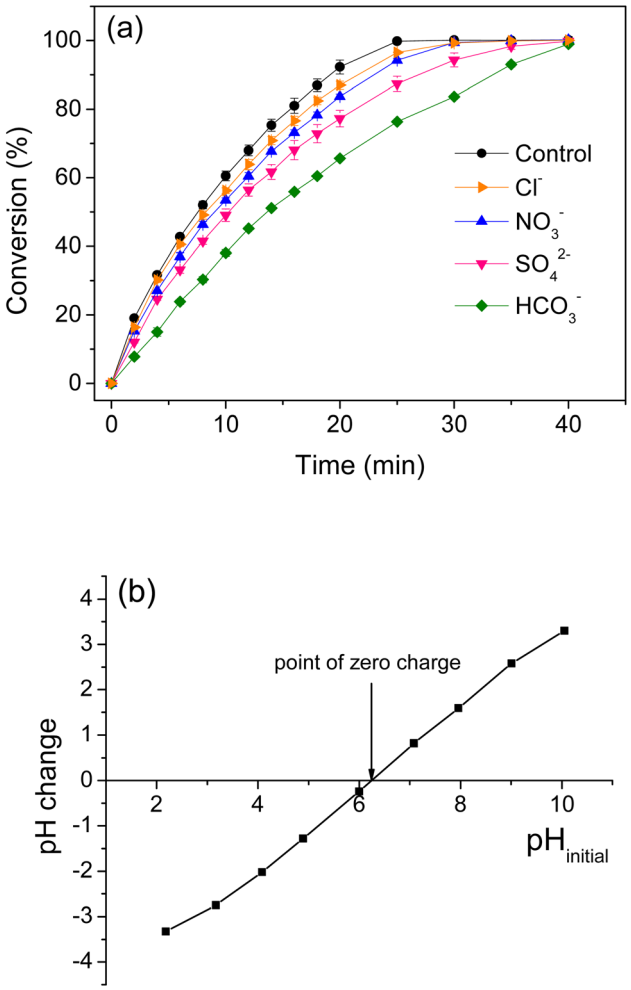

Fig. 11 (a) Effect of common anions (a). Condition: [cat.] = 3 g L^{-1}; [4-NP] = 15 mM; [$NaBH_4$] = 300 mM; [anion] = 5 mM. (b) Point of zero charge plot of HKUST-1 composite.

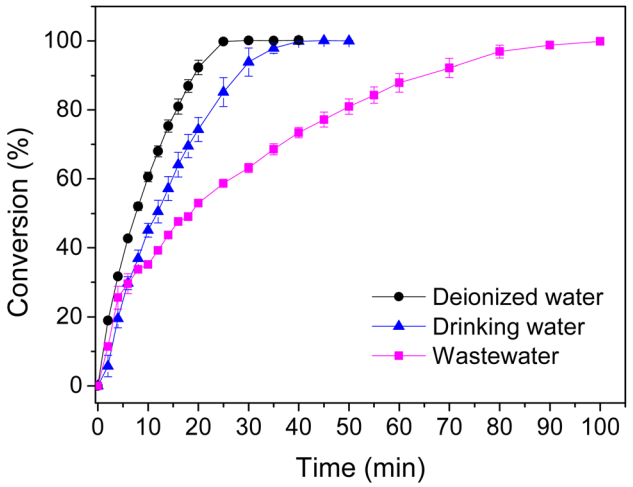

Fig. 12 Catalytic performance of HKUST-1 composite in actual water environment. Condition: [cat.] = 3 g L^{-1}; [4-NP] = 15 mM; [$NaBH_4$] = 300 mM.

and the catalyst.[4] The catalytic performances of other monometallic MOF-based catalysts for 4-NP reduction are summarized in Table 1. The HKUST-1 composite demonstrated performance comparable to that of the other catalysts, even when evaluated at a higher concentration of 4-NP.

3.2.6 Effect of anions. The effectiveness of the HKUST-1 composite catalyst was evaluated in the presence of common anions found in surface water, including Cl^-, NO_3^-, SO_4^{2-}, and HCO_3^-. The concentrations of these anions were 5 mM to mimic the sewage water.[37] As shown in Fig. 11(a), the presence of these anions slightly decreased the reduction rate; however, complete conversion was still observed within 40 minutes. The point of zero charge (PZC) of the HKUST-1 composite was determined using a pH drift method. Fig. 11(b) illustrates that the PZC was found to be 6.25. Under unadjusted pH conditions (pH = 5), the HKUST-1 composite was protonated and positively charged. The anions competed with nitrophenolate for adsorption on the positively charged surface of the catalyst, which resulted in a delay in the reduction process.[38]

3.2.7 Evaluation in actual water environments. The catalytic efficiency of the HKUST-1 composite catalyst was also assessed in real water environments. As displayed in Fig. 12, the conversion rate decreased with lower water purity. Factors such as the hydrophobicity of the water samples, their charge, and the presence of donor atoms influenced the reduction reaction.[39] Despite these variations, complete reduction was still achieved when tested in wastewater, indicating the practicality of the catalyst.

3.3 Reductions of other organic pollutants

The composite catalyst was also evaluated for the reduction of 2-NP and two azo dye models: methyl orange and Congo red. As displayed in Fig. 13(a), the absorbance of 2-NP at 415 nm declined over time. The UV-vis spectra for methyl orange are presented in Fig. 13(b). A reduction in the peak intensity at 465 nm of methyl orange, along with an increase in the peak intensity at 247 nm corresponding to sulfanilic acid (the reduction product), confirmed the occurrence of the reduction reaction.[40] The UV-vis spectra depicting the reduction of Congo red are illustrated in Fig. 13(c), where the peak intensity at 498 nm diminished over time due to the cleavage of the azo group, resulting in the formation of aromatic amines.[41] The decrease in the peak intensity was not attributed to the dye adsorption as the adsorption–desorption equilibrium was established before initiating the reduction process using $NaBH_4$. Fig. 13(d) shows the conversion rates of 4-NP, 2-NP, methyl orange, and Congo red over time. The reduction of 2-NP was slightly slower than that of 4-NP, with complete reduction achieved within 40 minutes. Furthermore, the composite catalyst successfully reduced 100% of methyl orange and 69% of Congo red. The k_{app} values for the reductions of 4-NP, 2-NP, methyl orange, and Congo red by the composite catalyst were 0.1008, 0.0845, 0.414, and 0.245, respectively (Fig. 13(e)).

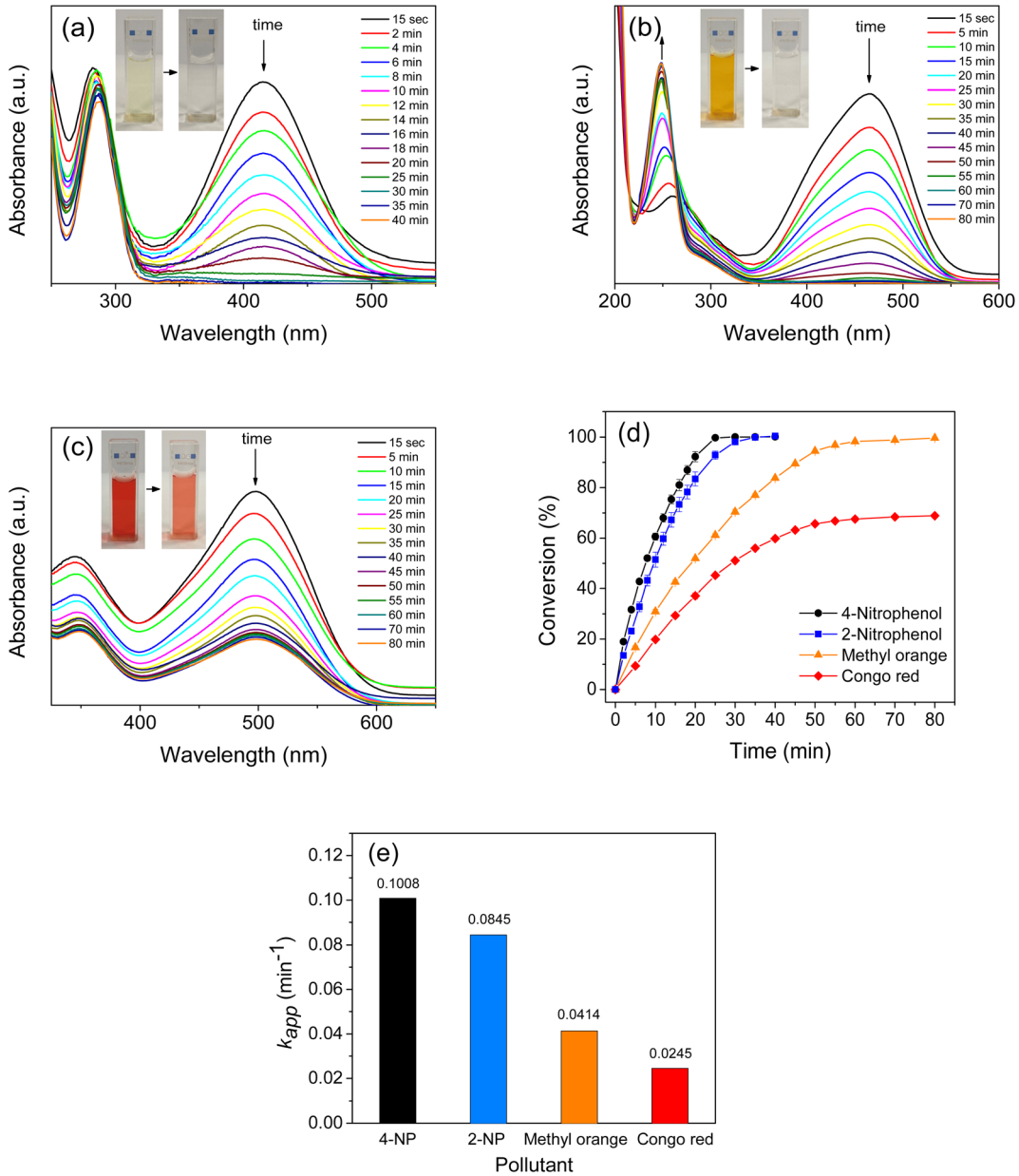

Fig. 13 UV-visible absorption spectra of 2-nitrophenol (a), methyl orange (b), and Congo red (c) reduced by HKUST-1 composite/$NaBH_4$ over time. The inset shows the change of color after reduction. (d) Catalytic performances of HKUST-1 composite and (e) rate constants for the reduction of pollutants. Condition: [cat.] = 3.0 g L^{-1}; [$NaBH_4$] = 300 mM; [pollutant] = 15 mM.

4. Conclusions

In this study, we demonstrated the reutilization of Cu^{2+}-adsorbed hydrogel as a catalyst for the reduction of 4-NP to 4-AP. The Cu^{2+} ions adsorbed in the hydrogel were transformed into HKUST-1 through an *in situ* synthesis process. The synthesis of HKUST-1 was characterized by FTIR, FESEM, and XPS analyses. TGA determined that the HKUST-1 content in the hydrogel was 11.2%. The HKUST-1 composite completely reduced the 4-NP solution within 25 minutes. The reduction rates increased at elevated temperatures, with the activation energy calculated to be 54.4 kJ mol^{-1}. When compared to other MOF-based catalysts for 4-NP reduction, the performance of our composite catalyst was competitive, even when evaluated at a higher concentration of 4-NP. Furthermore, the catalyst proved effective under ambient conditions, achieving a complete conversion of 4-NP. Finally, the composite catalyst demonstrated its capability to reduce other target organic pollutants, including 2-NP, methyl orange, and Congo red, and it could be easily separated *via* filtration.

Data availability

The manuscript includes all data supporting this article.

Conflicts of interest

There are no conflicts to declare.

Acknowledgements

This research was funded by the Fundamental Fund of Khon Kaen University, the National Science Research and Innovation Fund (NSRF), and Center of Excellence for Innovation in Chemistry (PERCH-CIC), Ministry of Higher Education, Science, Research and Innovation. The authors thank Panjalak Meetam and Jiraporn Pimphumee for their assistance with UV-vis and LC-MS measurements.

References

1 K. Zhao, J. Wang, W. Kong and P. Zhu, *J. Environ. Chem. Eng.*, 2020, **8**, 103517.
2 J. Shen, R. He, L. Wang, J. Zhang, Y. Zuo, Y. Li, X. Sun, J. Li and W. Han, *J. Hazard. Mater.*, 2009, **167**, 193–198.
3 A. B. Azzam, R. Djellabi, S. M. Sheta and S. M. El-Sheikh, *RSC Adv.*, 2021, **11**, 18797–18808.
4 F. Lin and R. Doong, *Appl. Catal., A*, 2014, **486**, 32–41.
5 Z.-S. Lv, X.-Y. Zhu, H.-B. Meng, J.-J. Feng and A.-J. Wang, *J. Colloid Interface Sci.*, 2019, **538**, 349–356.
6 T. M. Ansari, M. Ajmal, S. Saeed, H. Naeem, H. B. Ahmad, K. Mahmood and Z. H. Farooqi, *J. Iran. Chem. Soc.*, 2019, **16**, 2765–2776.
7 Y. R. Mejía and N. K. Reddy Bogireddy, *RSC Adv.*, 2022, **12**, 18661–18675.
8 P. Boonying, S. Martwiset and S. Amnuaypanich, *Appl. Nanosci.*, 2018, **8**, 475–488.
9 S. Jana, S. Ghosh, S. Nath, S. Pande, S. Praharaj, S. Panigrahi, S. Basu, T. Endo and T. Pal, *Appl. Catal., A*, 2006, **313**, 41–48.
10 M. Ajmal, M. Siddiq, H. Al-Lohedan and N. Sahiner, *RSC Adv.*, 2014, **4**, 59562–59570.
11 N. Sahiner and S. Sagbas, *Colloids Surf., A*, 2013, **418**, 76–83.
12 S. S.-Y. Chui, S. M.-F. Lo, J. P. H. Charmant, A. G. Orpen and I. D. Williams, *Science*, 1999, **283**, 1148–1150.
13 K.-Y. Andrew Lin and Y.-T. Hsieh, *J. Taiwan Inst. Chem. Eng.*, 2015, **50**, 223–228.
14 Y. Zhang, C. Qian, J. Duan, Y. Liang, J. Luo, Y. Han, J. Hu and F. Shi, *Appl. Surf. Sci.*, 2022, **573**, 151558.
15 J. Yu and Y. Sun, *J. Environ. Chem. Eng.*, 2024, **12**, 113051.
16 P. Meetam, K. Phonlakan, S. Nijpanich and S. Budsombat, *Int. J. Biol. Macromol.*, 2024, **255**, 128261.
17 K. Phonlakan, S. Pornsuwan, S. Nijpanich and S. Budsombat, *Int. J. Biol. Macromol.*, 2024, **265**, 130922.
18 A. Nachaichot, K. Phonlakan, S. Nijpanich, S. Pornsuwan and S. Budsombat, *RSC Adv.*, 2024, **14**, 35628–35637.
19 X. Cui, X. Sun, L. Liu, Q. Huang, H. Yang, C. Chen, S. Nie, Z. Zhao and Z. Zhao, *Chem. Eng. J.*, 2019, **369**, 898–907.
20 B. Di Credico, M. Redaelli, M. Bellardita, M. Calamante, C. Cepek, E. Cobani, M. D'Arienzo, C. Evangelisti, M. Marelli, M. Moret, L. Palmisano and R. Scotti, *Catalysts*, 2018, **8**, 353.
21 L. Zhang, J. Zheng, C. Zhang, Y. Wang, J. Zeng, H. He, T. Yuan, Y. Qin and Y. Zheng, *Trans. Nonferrous Met. Soc. China*, 2022, **32**, 251–261.
22 P. Jagódka, K. Matus and A. Łamacz, *Molecules*, 2022, **27**, 7082.
23 Y. Wang, Y. Lü, W. Zhan, Z. Xie, Q. Kuang and L. Zheng, *J. Mater. Chem. A*, 2015, **3**, 12796–12803.
24 Y. Wang, J. Wang, Z. Yuan, H. Han, T. Li, L. Li and X. Guo, *Colloids Surf., B*, 2017, **152**, 252–259.
25 R. Shi, C. Liu, W. Wang, N. Wang, P. Shen, Z. Liu, J. Hu and F. Shi, *Mater. Lett.*, 2023, **352**, 135177.
26 E. Aykut, M. Sert and E. Sert, *J. Water Process Eng.*, 2023, **54**, 103970.
27 S. Wunder, F. Polzer, Y. Lu, Y. Mei and M. Ballauff, *J. Phys. Chem. C*, 2010, **114**, 8814–8820.
28 A. Feng, C. Lin, H. Zhou, W. Jin, Y. Hu, D. Li and Q. Li, *Green Chem. Eng.*, 2024, **5**, 205–212.
29 A. Venkateshaiah, D. Silvestri, R. K. Ramakrishnan, S. Wacławek, V. V. T. Padil, M. Černík and R. S. Varma, *Molecules*, 2019, **24**, 3643.
30 A. V. Churikov, I. M. Gamayunova, K. V. Zapsis, M. A. Churikov and A. V. Ivanishchev, *Int. J. Hydrogen Energy*, 2012, **37**, 335–344.
31 T. K. Das and N. Ch. Das, *Int. Nano Lett.*, 2022, **12**, 223–242.
32 G. K. Parshetti and R. Doong, *Chemosphere*, 2012, **86**, 392–399.
33 A. Ehsani, S. Nejatbakhsh, A. M. Soodmand, M. E. Farshchi and H. Aghdasinia, *Environ. Res.*, 2023, **227**, 115736.
34 Md. A. Ahsan, E. Deemer, O. Fernandez-Delgado, H. Wang, M. L. Curry, A. A. El-Gendy and J. C. Noveron, *Catal. Commun.*, 2019, **130**, 105753.
35 P. Karthik, A. Pandikumar, M. Preeyanghaa, M. Kowsalya and B. Neppolian, *Microchim. Acta*, 2017, **184**, 2265–2273.
36 J. Li, X. Sun, S. Subhan, W. Gong, W. Li, W. Sun, Y. Zhang, M. Lu, H. Ji, Z. Zhao and Z. Zhao, *Chem. Eng. J.*, 2022, **446**, 137314.
37 S. Bo, X. Zhao, Q. An, J. Luo, Z. Xiao and S. Zhai, *RSC Adv.*, 2019, **9**, 5009–5024.
38 T. Aditya, J. Jana, N. K. Singh, A. Pal and T. Pal, *ACS Omega*, 2017, **2**, 1968–1984.
39 L. Sun, J. He, S. An, J. Zhang, J. Zheng and D. Ren, *Chin. J. Catal.*, 2013, **34**, 1378–1385.
40 A. Mondal, B. Adhikary and D. Mukherjee, *Colloids Surf., A*, 2015, **482**, 248–257.
41 E. A. Bakr, M. N. El-Nahass, W. M. Hamada and T. A. Fayed, *RSC Adv.*, 2021, **11**, 781–797.